Available online at www.sciencedirect.com
SCIENCE DIRECT®
International Journal of Mass Spectrometry 229 (2003) 77–82
International Journal of Mass Spectrometry
www.elsevier.com/locate/ijms

Band gap shiftings in Co-doped Nb_n ($n = 3$–15) clusters: influence of Co 3d electrons on the electronic structure

Axel Pramann [a], Kiichirou Koyasu [a], Atsushi Nakajima [a,*], Koji Kaya [b]

[a] *Department of Chemistry, Faculty of Science and Technology, Keio University, 3-14-1 Hiyoshi, Kohoku-ku, Yokohama 223-8522, Japan*
[b] *Institute of Molecular Science, Myodaiji, Okazaki 444-8585, Japan*

Received 15 February 2003; accepted 10 March 2003

Abstract

The photoelectron spectra of bimetallic, mass-selected Nb_nCo^- clusters ($n = 3$–15) measured at 4.66 eV photon energy are reported. The electronic structure changes of the binary clusters are discussed in comparison with the electronic structures of pure Nb_n^- clusters as a function of size evolution. Spectroscopic parameters like electron affinities (EAs) and vertical detachment energies (VDEs) are determined. The addition of one Co atom to the Nb_n cluster core significantly perturbs the electronic structures of pure Nb_n clusters at small cluster sizes. Electronic state merging can be explained by hybridization of Co 3d and 4s as well as Nb_n 4d-derived valence orbitals. Tentative geometric structure postulations are carried out revealing the influence of the incoming Co atom toward the intact Nb_n cluster core. In strong contrast to pure Nb_n clusters, a highest occupied molecular orbital–lowest unoccupied molecular orbital (HOMO–LUMO) gap closing of Nb_nCo at $n = 6$ indicates a bulk-like evolution of electronic structures induced by charge transfer of Co 3d electrons.

Keywords: HOMO-LUMO gap; Band gap shifting; Electron affinity

1. Introduction

In contrast to pure metal clusters, bimetallic or alloy clusters are less-intense studied, but have become a matter of increasing research activity and importance [1–10]. The basic idea is related to the valuable role of bimetallic surfaces in heterogeneous catalysis and chemisorption processes [11–14]. Special properties like reactivity and selectivity can be taylored as a function of particle size and composition. To gain primary insight into these microscopic interactions it is of fundamental interest to study properties like electronic or geometric structures from small systems toward bulk phase adding atom by atom.

Some examples show that geometric and electronic structures can be further correlated with other size-dependent properties. Especially rates of reactions of bimetallic clusters toward small molecules like H_2 have been compared to the size evolution of structure. One of the first studies in this area is an attempt of the correlation of hydrogen chemisorption rates and ionization potentials (IPs) in pure neutral iron clusters [15]. Furthermore, ionization threshold energies of Nb_n clusters and their chemisorption rates toward D_2 have revealed a considerable correlation [16]. Another approach has been implemented in a direct correlation between a chemisorption barrier and cluster electron promotion energies, the latter determined from differences of IPs and EAs [17]. This method is adopted from solid surfaces and has been successfully applied in the case of pure iron, cobalt, and nickel clusters, and recently for Nb clusters [17,18]. However, this model is not generally applicable to bimetallic clusters as has been demonstrated in the case of $Co_nV_m^-$ clusters [19].

Recently, our group has enforced the study of size-dependent evolution of the electronic structure of bimetallic clusters using anion photoelectron spectroscopy [19–22]. Actually, in most cases both geometric factors as well as electronic properties coincide in responsibility for their very size-dependent reactivity [23]. Another fascinating approach to gain insight into the geometries of small bimetallic clusters is the application of chemical probe studies [5,7]. As a result, these studies show that the investigation of combined properties like reactivity and electronic structure provides

* Corresponding author. Tel.: +81-45-566-1712; fax: +81-45-566-1697.
E-mail address: nakajima@sepia.chem.keio.ac.jp (A. Nakajima).

1387-3806/$ – see front matter © 2003 Elsevier B.V. All rights reserved.
doi:10.1016/S1387-3806(03)00258-6

a deeper understanding in processes on a sub-nanometer scale as a function of size and composition.

In this paper, the size-dependent evolution of the electronic structure of small bimetallic Nb_nCo^- ($n = 3$–15) clusters is reported for the first time using anion photoelectron spectroscopy with a detachment energy of 4.66 eV. By comparing the electronic structures of bimetallic Nb_nCo clusters with those of pure Nb_n clusters as a function of size, the influence of a single Co atom toward the electronic structure change is directly observed. In a first approach, the kind of chemical bonding between Co and the Nb_n cluster is treated with a simple charge-transfer model. The latter enables us to explain the chemical bonding by hybridization of the respective orbitals of Co and the Nb_n clusters.

2. Experiment

The cluster beam apparatus, the anion photoelectron spectrometer as well as the applied methods have been described in a previous paper [24]. Here, only a short overview is presented. Bimetallic Nb_nCo^- clusters are generated using a double rod pulsed laser vaporization cluster source [2,3]. The light of the second harmonics output (532 nm, 10 Hz repetition rate) of two Nd^{3+}:YAG lasers is focused onto rotating and translating Nb and Co rods. Cluster formation is carried out by cooling the dense metal plasma with a high pressure pulse of helium (10 atm, provided by a pulsed solenoid valve) in a 2 mm diameter channel of 20 mm length (cooling with liquid N_2 is optional, but not performed during this work). The clusters then undergo an adiabatic supersonic expansion. Negatively charged clusters are mass-analyzed according to their mass/charge ratios with the aid of an in-line time-of-flight mass spectrometer (TOF-MS) with a resolution $m/\Delta m = 230$. This resolution is sufficient in the investigated mass range to separate between clusters of interest and oxide impurities. Furthermore, the mass-selected clusters are decelerated using a technique invented by Handschuh et al. [25]. This step is crucial to reduce the signal broadening caused by the Doppler effect. After arriving at the detachment region of the time-of-flight magnetic bottle-type photoelectron spectrometer (TOF-PES) [26–28], a second pulse of the fourth harmonics output of another Nd^{3+}:YAG laser (laser fluence: 1–2 mJ/cm^2) is focused onto the cluster anions of selected size. The kinetic energy distribution of the ejected photoelectrons is measured via their flight times. Subsequently, the electron kinetic energy (eKE) spectra are converted to electron binding energy (eBE) spectra using the relation: $eBE = h\nu - eKE$. Calibration of the TOF-PES is carried out using the strong $^1S_0 \rightarrow {}^2S_{1/2}$ and $^1S_0 \rightarrow {}^2D_{5/2}$ lines of the gold atomic anion [29]. In the current study, the resolution of the TOF-PES is better than 50 meV at 1 eV eKE, which decreases at higher eKE according to $eKE^{3/2}$. The spectra are recorded by accumulating 10,000–30,000 events at 10 Hz repetition rate. It is important to mention that the PE spectral shapes exhibit no changes as a function of the detachment laser power.

3. Results and discussion

3.1. Mass spectra of Nb_nCo^-

A typical TOF mass spectrum of bimetallic Nb_nCo^- clusters is shown in Fig. 1. The maximum of the mass distribution is located at $n = 5$. Pure Nb_n^- as well as $Nb_nO_m^-$ ($m = 1, 2$) clusters show highest intensities. The oxide impurities result from the high oxygen affinity of early transition metal clusters. In the current study, single Co-doped Nb_n^- clusters reveal highest intensities under the bimetallic series. Nb_nCo^- clusters are the only bimetallic Nb- and Co-containing species we are able to study, because of the minor intensity of clusters with higher Co content. Additionally, the inset shows a more detailed part of the mass spectrum around the Nb_5^- and Nb_6^- cluster. Each series of pure Nb_n^- clusters is accompanied by monoxides, dioxides, and single Co-doped binary clusters.

3.2. Photoelectron spectroscopy of Nb_nCo^- clusters

The photoelectron spectra of pure Nb_n^- and Nb_nCo^- clusters are displayed in Figs. 2 and 3. All spectra are measured at 4.66 eV photon energy. As a general approach, the photodetachment process reveals the electronic transitions from the ground state of the anionic cluster to the ground or excited states of the corresponding neutral cluster in the geometry of the anion. A strong broadening near the threshold refers to a geometric reordering between the structures

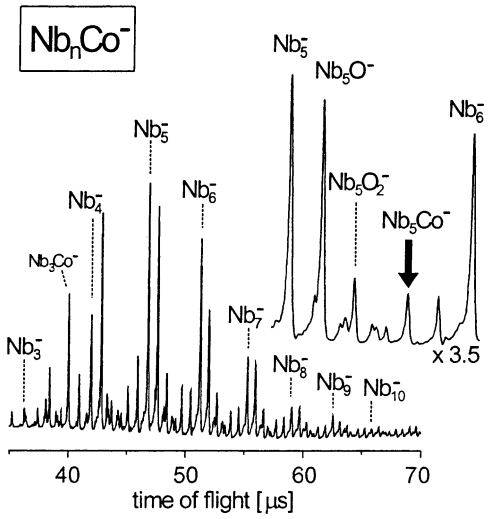

Fig. 1. Typical time-of-flight mass spectrum of Nb_nCo^- clusters in the size range $n = 3$–10. The inset shows the respective satellite peaks in the case of the pentamer. Each Nb_n^- cluster is accompanied by the corresponding monoxide and dioxide. Bimetallic $Nb_nCo_m^-$ clusters of sufficient intensity are obtained for Nb_nCo^-.

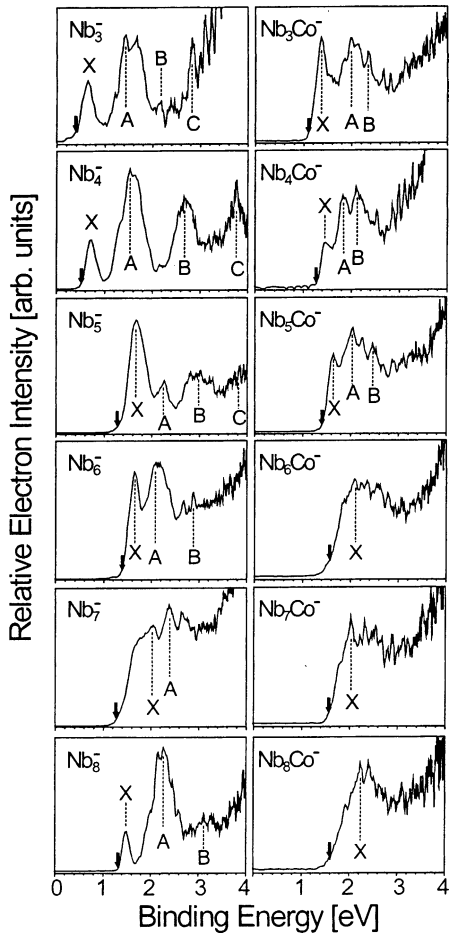

Fig. 2. Photoelectron spectra of pure Nb_n^- ($n = 3$–8) clusters measured at 4.66 eV photon energy (left column). PE spectra of Nb_nCo^- clusters ($n = 3$–8) (right column). Spectral features of Nb_n^- clusters correspond to those reported in [18,30]. Downward arrows indicate EAs (for details, see text).

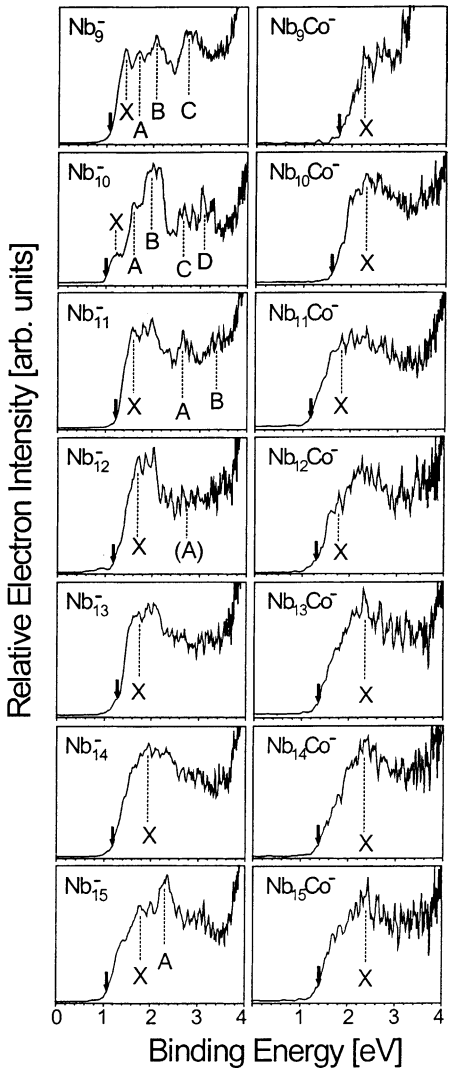

Fig. 3. Photoelectron spectra of pure Nb_n^- ($n = 9$–15) clusters measured at 4.66 eV photon energy (left column). PE spectra of Nb_nCo^- clusters ($n = 9$–15) (right column). Spectral features of Nb_n^- clusters correspond to those reported in [18]. Downward arrows indicate EAs (for details, see text).

of the anion and the neutral. In this work, threshold binding energies are determined by taking the binding energy at 10% of the first peak maximum. These threshold energies are treated as upper limits of EAs. The latter are only accessible when vibrational progressions of the ground state transition can be resolved. Furthermore, vertical detachment energies (VDEs) are measured by taking the binding energy of the maximum of the corresponding peaks. Fig. 4 shows the electron affinities (EAs) and corresponding 1.VDEs of Nb_n and Nb_nCo clusters.

In Figs. 2 and 3 the relative electron intensities are plotted versus the eBE. The spectra of Nb_n^-—shown as a reference—are measured under the same experimental conditions as the bimetallic clusters. Thus, effects of electronic structural changes due to the additional Co atom are easy to observe. Generally, the spectral features of pure Nb_n^- clusters correspond to those reported in [18,30]. The downward arrows denote the EAs, and the labeling X, A, B, ... indicates the electronic transitions from the ground state of the anion to the ground state, first, second, ... excited state of the neutral clusters. Generally, even at a photon energy of 4.66 eV the spectra show structured features. This is a direct consequence of the valence electronic configuration of the niobium atoms ($[Kr]4d^45s^1$). In a detailed study of Nb_n clusters [18], the pure Nb_n clusters exhibit a clear size-dependent highest occupied molecular orbital–lowest unoccupied molecular orbital (HOMO–LUMO) energy gap variation as a consequence of the electron shell closings. Our investigation of the Nb_nCo^- clusters starts with the trimer ($n = 3$) series, because Nb_3Co^- is the smallest cluster which can be observed in the mass spectra under the current experimental conditions.

The spectrum of Nb_3^- reveals a HOMO-LUMO gap of 790 meV. According to a combined experimental/theoretical study by Ganteför and co-workers [30], a C_{2v} symmetry (trigonal planar structure) is proposed. The addition of one

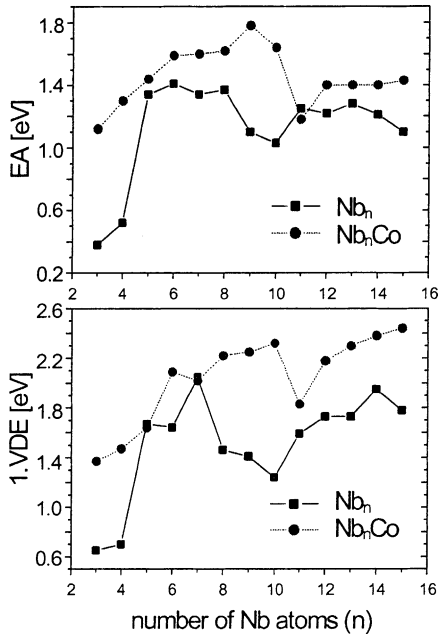

Fig. 4. Upper plot: electron affinities of Nb_n clusters (solid squares) and Nb_nCo clusters (solid circles). Lower plot: 1.vertical detachment energies of Nb_n clusters (solid squares) and Nb_nCo clusters (solid circles). Error bars (<150 meV) are not shown for more clarity.

Co atom changes the electronic structure strongly. The EA shifts about 740 meV toward higher binding energies. Additionally, the distance of the A and B bands merges significantly due to the hybridization of Co 3d and Nb 4d-derived molecular orbitals (MOs). The spectrum of the Co-doped Nb_3Co cluster exhibits a sharp onset with a strong first ground state transition (X). This is a clear indication of a rigid geometric structure—presumably a tetrahedron (D_{2d}) with slight distortion.

A much stronger influence toward the electronic structure by adding one Co atom can be observed by comparing the spectra of Nb_4^- and Nb_4Co^-. Whereas the PE spectrum of the pure Nb_4^- cluster reveals at least four distinct electronic bands according to a tetrahedral geometric structure [30], the addition of one Co atom causes a threshold shift of 780 meV. Additionally, the energy gaps between the bands are strongly merging. The large number of 3d electrons of the Co atom ($[Ar]3d^74s^2$) causes an enhancement of low-lying excited electronic states. The stability of one rigid isomer of the geometric structure of Nb_4Co^- is lowered compared to that of Nb_3Co^-. This is indicated by a less-intense first transition (X). However, the sharp onset and increase in EA might favor a distorted trigonal bipyramidal structure (distorted Nb_4 tetrahedron with a Co atom on a Nb_3 plane). In Nb_5, a prominent first peak (ground state transition X) at 1.67 eV dominates the spectrum. In [30], a distorted trigonal bipyramid is calculated. The Nb_5Co^- spectrum shifts only 100 meV toward higher binding energy (BE), but the HOMO-LUMO gap (410 meV) decreases about 190 meV. From $n = 5$, the PE spectra of Nb_nCo^- become rather similar as a result of an increase of the density of states (DOS) near the threshold. The hexamer series shows as a main feature a complete merging of the HOMO-LUMO gap in Nb_6Co. Regarding the gap of 450 meV in the Nb_6^- cluster, one additional Co atom now completely closes the gap. From $n = 6$, higher electronic states in the Nb_nCo^- clusters cannot be resolved under the current experimental conditions. The spectra of Nb_7^- and Nb_7Co^- are rather similarly structured. Whereas the most plausible geometric structure of Nb_7^- is a distorted pentagonal bipyramid [30], there are a number of plausible isomers available for Nb_7Co^-. The PE spectra of the octamer series Nb_8^- and Nb_8Co^- reveal rather different electronic structures. Nb_8 reveals a considerable large HOMO-LUMO gap of 760 meV which indicates a very stable geometric structure at a first glance. A recent, very detailed study on the electronic structure of the Nb_8^- cluster has been performed by Marcy and Leopold [31]. This group has applied vibrationally resolved negative ion photoelectron spectroscopy. In that study, the X-labeled peak of Nb_8 shows clear vibrational progressions. Marcy and Leopold suggest a C_{2v} structure as a geometry of lowest energy [31]. The incoming additional Co atom perturbs the electronic structure of the Nb_8 cluster drastically. The large HOMO-LUMO gap of 760 meV in Nb_8 merges completely, and a more smooth onset in the spectrum of Nb_8Co^- indicates a vibrational progression in the low energy side of the shoulder of the X band which cannot be resolved under the current experimental conditions. From $n = 9$, the Nb_nCo^- spectra become more similar in their electronic patterns, although local variations in threshold energies are observed. All spectra are dominated by an intense band (X), centered around 2 eV binding energy. In comparison, the PE spectrum of Nb_9^- shows a more structured electronic progression than that of Nb_9Co^- with an EA of 1.1 eV. One additional Co atom shifts the threshold about 680 meV toward higher binding energies. Even at $n = 10$, a well-structured electronic pattern can be observed for the pure Nb_{10} cluster—again revealing a much lower onset (1.03 eV) than in $Nb_{10}Co$ (1.64 eV). The spectra of Nb_{11}^- and $Nb_{11}Co^-$ are rather similar. A very broad band gap of 1 eV in Nb_{11} suggests a rigid geometric structure. For $n \geq 12$, the Nb_n^- and Nb_nCo^- spectra are dominated by a broad band (X) with a similar course. In this size range, the influence of the additional Co atom is of minor relevance. Here, the main spectral features are related to the Nb_n cluster core.

Fig. 4 shows the EAs (upper plot) and 1.VDEs (lower plot) of pure Nb_n clusters (solid squares) and Nb_nCo clusters (solid circles) for $n = 3$–15. Between $n = 4$ and 5 the EAs of the Nb_n clusters suddenly increase by 800 meV. A possible reason for this jump is a change between a two- and three-dimensional structure at this size. Whereas the cores of EAs slightly decrease up to $n = 10$ for Nb_n, a reverse trend—an increase of EAs—can be observed up to $n = 9$ in the case of Nb_nCo. These reverse directions in the EA evolution indicates a more delocalized bonding of the extra electron in Co-doped clusters, whereas in pure Nb_n

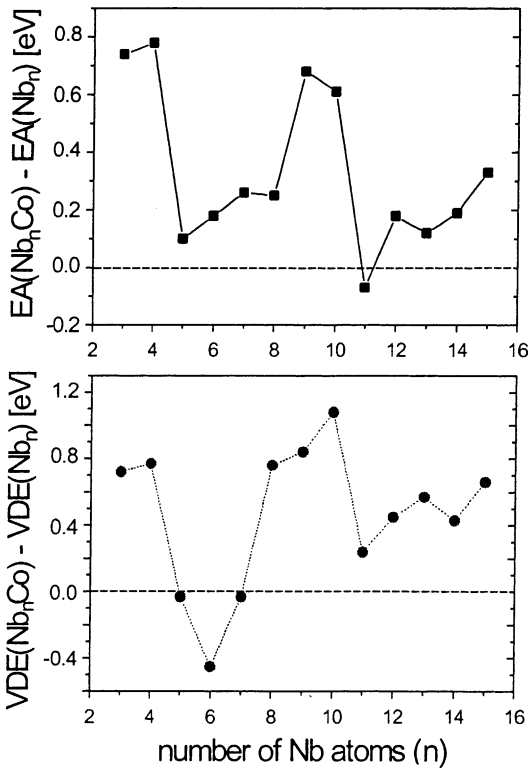

Fig. 5. Threshold shift direction indicated by differences of EAs (upper plot) and VDEs (lower plot) between bimetallic Nb_nCo and pure Nb_n clusters. The horizontal dashed line indicates conservation of threshold energies after Co doping.

clusters the extra electron is more localized. This trend can be observed in the VDEs of $n = 7$–10.

A more clear insight into binding energy shifts can be obtained by comparing the differences of EAs and VDEs of Nb_nCo and Nb_n clusters as is shown in Fig. 5. In the upper plot the difference $EA(Nb_nCo) - EA(Nb_n)$ is shown versus cluster size *n*, whereas the lower plot exhibits the respective differences of the 1.VDEs. The dashed line at $\Delta EA = 0$ and $\Delta VDE = 0$ indicates the conservation of EAs and VDEs after the addition of an Co atom. First, most EA differences are positive (except for $n = 11$). This additionally indicates a higher stability of Co-doped negatively charged Nb_n clusters compared to pure clusters due to a higher degree of electron delocalization induced by the size of the extra Co atom. Moreover, both the EA differences and the VDE differences reveal a strong decrease from $n = 4$ to 5, and at $n = 10$ to 11. The overall course of EA and VDE differences is similar. After the strong decrease in ΔEA and ΔVDE an increase is observed in the medium size range between $n = 5$ and 10 (EAs), and $n = 6$ and 11 (VDEs). For $n \geq 11$ both differences reveal local alternations.

In a first qualitative attempt, bonding between the Nb_n cluster core and the additional Co atom can be understood with the aid of an electron charge-transfer frontier orbital approach [32]: the respective electrons of valence MOs of the Nb_n cluster are transferred to atomic orbitals (AOs) of the Co atom, and a new set of MOs is generated. At first, electrons are directed from the Co 4s AO to a 5s- or 4d-derived LUMO of the corresponding neutral Nb_n cluster core. The reverse electron charge-transfer occurs from a Nb_n 4d-derived HOMO to an empty Co 3d AO which initially completes bonding between the niobium cluster and the Co atom. The strong variations in HOMO-LUMO gaps of Nb_n clusters in the investigated size range is a proof of a more covalent bonding character between the respective Nb atoms [18]. A completely different picture evolves for the Nb_nCo clusters: whereas a significant HOMO-LUMO gap separation can be observed up to $n = 5$, this very gap is merged for larger clusters, progressing toward bulk-phase electron emission spectra revealing increasing shifts of threshold energies. As a main result of the current study, the addition of only one Co atom to the Nb_n cluster causes a bulk-like electronic structure at a very small cluster size. However, exact predictions about the electronic states can be made only in coincidence with accurate theoretical structure calculations.

4. Conclusions

We report a photoelectron spectroscopic study of small mass-selected Nb_nCo^- ($n = 3$–15) clusters for the first time. The Nb_nCo^- clusters are produced by a pulsed double rod laser vaporization cluster source. PE spectra are measured at 4.66 eV (266 nm) photon energy with the aid of a magnetic bottle-type photoelectron spectrometer. This study provides information about the evolution of the electronic structure of Nb_nCo clusters as a function of size and in comparison with pure Nb_n clusters. EAs and VDEs are determined. Generally, the addition of one Co atom strongly perturbs the electronic structure of the Nb_n cluster core. The interaction between the incoming Co atom and the Nb_n cluster core can be described via a frontier orbital electron charge transfer. Distinct HOMO-LUMO gaps in pure Nb_n clusters merge after the addition of one Co atom by an increase of low energetic excited states. Therefore, the doping of small Nb_n clusters with one Co atom generates a bulk-like electronic structure for Nb_nCo at already $n = 6$. This gap-closing by just one heterometal atom might provide new forthcoming materials in semiconductor research.

Acknowledgements

This work is supported by a program entitled “Research for the Future (RFTF)” of the Japan Society for the Promotion of Science (98P01203) and by a Grant-in-Aid for scientific research (C) (No. 13640582) and for the 21st Century COE program “KEIO Life Conjugate Chemistry” from the Ministry of Education, Culture, Sports, Science and Technology. A.P. gratefully acknowledges a postdoctoral fellowship from the Japan Society for the Promotion of Science (JSPS).

References

[1] T.G. Taylor, K.F. Willey, M.B. Bishop, M.A. Duncan, J. Phys. Chem. 94 (1990) 8016.
[2] S. Nonose, Y. Sone, K. Onodera, S. Sudo, K. Kaya, J. Phys. Chem. 94 (1990) 2744.
[3] A. Nakajima, T. Kishi, T. Sugioka, Y. Sone, K. Kaya, J. Phys. Chem. 95 (1991) 6833.
[4] R.L. Wagner, W.D. Vann, A.W. Castleman Jr., Rev. Sci. Instrum. 68 (1997) 3010.
[5] E.K. Parks, K.P. Kerns, S.J. Riley, Chem. Phys. 262 (2000) 151.
[6] W. Bouwen, P. Thoen, F. Vanhoutte, S. Boukaert, F. Despa, H. Weidele, R.E. Silverans, P. Lievens, Rev. Sci. Instrum. 71 (2000) 54.
[7] G.M. Koretsky, K.P. Kerns, G.C. Nieman, M.B. Knickelbein, S.J. Riley, J. Phys. Chem A 103 (1999) 1997 (and references therein).
[8] U. Heiz, A. Vayloyan, E. Schumacher, C. Yeretzian, M. Stener, P. Gisdakis, N. Roesch, J. Chem. Phys. 105 (1996) 5574.
[9] O.C. Thomas, W.-J. Zheng, K.H. Bowen Jr., J. Chem. Phys. 114 (2001) 5514.
[10] O.C. Thomas, W.-J. Zheng, T.P. Lippa, S.-J. Xu, S.A. Lyapustina, K.H. Bowen Jr., J. Chem. Phys. 114 (2001) 9895.
[11] J.H. Sinfelt, Bimetallic Catalysis: Discoveries, Concepts, and Applications, Wiley, New York, 1983.
[12] B.E. Koel, G.A. Somorjai, in: J.R. Anderson, M. Boudart (Eds.), Catalysis, Springer-Verlag, Berlin, 1985.
[13] D.M. Zehner, D.M. Goodman (Eds.), Physical and Chemical Properties of Thin Metal Overlayers and Alloy Surfaces, Mater. Res. Soc. 83 (1987).
[14] J.A. Rodriguez, Surf. Sci. Rep. 24 (1996) 223.
[15] R.L. Whetten, D.M. Cox, D.J. Trevor, A. Kaldor, Phys. Rev. Lett. 54 (1985) 1494.
[16] R.L. Whetten, M.R. Zakin, D.M. Cox, D.J. Trevor, A. Kaldor, J. Chem. Phys. 85 (1986) 1697.
[17] J. Conceicao, R.T. Laaksonen, L.-S. Wang, T. Guo, P. Nordlander, R.E. Smalley, Phys. Rev. B 51 (1995) 4668.
[18] H. Kietzmann, J. Morenzien, P.S. Bechthold, G. Ganteför, W. Eberhardt, J. Chem. Phys. 109 (1998) 2275.
[19] A. Pramann, K. Koyasu, A. Nakajima, K. Kaya, J. Phys. Chem. A 106 (2002) 2483.
[20] Y. Negishi, Y. Nakamura, A. Nakajima, K. Kaya, J. Chem. Phys. 115 (2001) 3657.
[21] A. Pramann, A. Nakajima, K. Kaya, J. Chem. Phys. 115 (2001) 5404.
[22] A. Pramann, A. Nakajima, K. Kaya, Chem. Phys. Lett. 347 (2001) 366.
[23] W.J.C. Menezes, M.B. Knickelbein, Chem. Phys. Lett. 183 (1991) 357.
[24] A. Nakajima, T. Taguwa, K. Hoshino, T. Sugioka, T. Naganuma, F. Ono, K. Watanabe, K. Nakao, Y. Konishi, R. Kishi, K. Kaya, Chem. Phys. Lett. 214 (1993) 22.
[25] H. Handschuh, G. Ganteför, W. Eberhardt, Rev. Sci. Instrum. 66 (1995) 3838.
[26] P. Kruit, F.H. Read, J. Phys. E 16 (1983) 313.
[27] O. Cheshnovsky, S.H. Yang, C.L. Pettiette, M.J. Craycraft, R.E. Smalley, Rev. Sci. Instrum. 58 (1987) 2131.
[28] G. Ganteför, K.-H. Meiwes-Broer, H.O. Lutz, Phys. Rev. A 37 (1988) 2716.
[29] H. Hotop, W.C. Lineberger, J. Phys. Chem. Ref. Data 4 (1975) 539.
[30] H. Kietzmann, J. Morenzien, P.S. Bechthold, G. Ganteför, W. Eberhardt, D.-S. Yang, P.A. Hackett, R. Fournier, T. Pang, C. Chen, Phys. Rev. Lett. 77 (1996) 4528.
[31] T.P. Marcy, D.G. Leopold, Int. J. Mass Spectrom. 195/196 (2000) 653.
[32] J.-Y. Saillard, R. Hoffman, J. Am. Chem. Soc. 106 (1984) 2006.